

Rover Autonomy for Long Range Navigation and Science Data Acquisition on Planetary Surfaces

Terry Huntsberger, Hrand Aghazarian, Yang Cheng, Eric T. Baumgartner, Edward Tunstel, Chris Leger, Ashitey Trebi-Ollennu, and Paul S. Schenker

Jet Propulsion Laboratory, California Institute of Technology
4800 Oak Grove Drive, Pasadena, CA 91109-8099

{terry,hrand,ycheng,ericb,tunstel,cleger,ashitey,schenker}@telerobotics.jpl.nasa.gov

ABSTRACT

This paper describes recent work undertaken at the Jet Propulsion Laboratory in Pasadena, CA in the area of increased rover autonomy for planetary surface operations. The primary vehicle for this work is the Field Integrated, Design and Operations (FIDO) rover. The FIDO rover is an advanced technology prototype that is a terrestrial analog of the Mars Exploration Rovers (MER) being sent to Mars in 2003. We address the autonomy issue through improved integration of rover based sensing and higher level onboard planning capabilities. The sensors include an inertial navigation unit (INU) with 3D gyros and accelerometers, a sun sensor, mast and body mounted imagery, and wheel encoders. Multisensor fusion using an Extended Kalman Filter (EKF) approach coupled with pattern recognition and tracking algorithms has enabled the autonomy that is necessary for maximizing science data return while minimizing the number of ground loop interactions. These algorithms are coupled with a long range navigation algorithm called ROAMAN (Road Map Navigation) for an integrated approach to rover autonomy. We also report the results of algorithm validation studies in remote field trials at Black Rock Summit in Central Nevada, California's Mojave Desert, and the Arroyo Seco at JPL.

1 INTRODUCTION

There are a number of autonomy issues that need to be addressed prior to the long duration rover mission to Mars that are being planned by NASA/JPL for 2009 and beyond. Among these are navigation to destinations possibly hundreds of meters away that are beyond the range of mast mounted sensors, precision rendezvous with both man-made (landers) and natural targets, and autonomous, collision-free deployment of arm mounted science instruments. The Field Integrated Design and Operations (FIDO) rover team at the Jet Propulsion Laboratory in Pasadena, CA has developed a suite of algorithms that address these autonomy issues. These algorithms have been tested on the FIDO rover in various remote outdoor environments that serve as a terrestrial analog to Mars. Since 1999, JPL has been developing the FIDO rover – an advanced technology rover that in many ways is a terrestrial analog of the Mars Exploration Rover, also called MER, that will fly to Mars in 2003. FIDO comes equipped

The research described in this paper was carried out at the Jet Propulsion Laboratory, California Institute of Technology, under a contract with the National Aeronautics and Space Administration. (address all correspondence to Terry Huntsberger, telephone: 818-354-5794, e-mail: terry@telerobotics.nasa.gov).

with a host of scientific instruments and is capable of traversing long distances for extended in-situ exploration.

Traditional approaches to rover navigation follow a sense/plan/act strategy that usually requires long time delays between movement and relatively large computational resources. The vehicles successfully used previously, such as the CMU NAVLAB or JPL Robby projects, massed between two to three tons and required 300 to 500 MIPs of processing power. The mass and power requirements of long range rover missions preclude the use of such a strategy. These concerns were addressed by subsequent studies undertaken at JPL using reactive methods [1]. Purely reactive methods tend to suffer from deadlock and trapping conditions if no longer range path planning is used.

There have been numerous efforts to develop algorithms for long range navigation that are both efficient and that address the trapping problem. Among these are the systems developed at CMU for efficient path planning during long range traverses [6, 10, 14, 15], variants of the tangent-bug algorithms [5, 16, 17], and C-space approaches [2, 13]. We have developed an algorithm called ROAMAN (Road Map Navigation) that combines the compactness of the C-space representation of the environment with the efficiency of the path search algorithms such as D* [14]. The algorithm has been implemented on the FIDO rover and field tested at various remote sites.

These field trials with the FIDO rover have indicated that there is a great amount of slippage in the drive wheels during traversal of Mars analog terrain. This precludes the use of purely dead-reckoning techniques for navigation and obstacle avoidance. This point was recently addressed by Baumgartner, et al. [8, 9, 11] using an extended Kalman filter (EKF) integration of wheel odometry, inertial navigation unit gyros, and sun sensor [3] inputs to refine the dead reckoning position estimates. Their system accurately localized a rover in the laboratory to within 1%. These are similar to the results also obtained by Volpe [4] in long-range mission scenario field trials on Rocky 7, another prototype Mars rover at NASA-JPL. All of the turn-in-place maneuvers on FIDO are done under EKF control since heading errors quickly propagate during subsequent straight-line traverses.

The sections of this paper that follow are organized as follows: Section 2 presents a brief description of the FIDO rover. This is followed by descriptions of ROAMAN, long-range

rendezvous with man-made targets, and short-range rendezvous with natural science target in Sections 3, 4, and 5 respectively. The experimental studies are described in Section 7, and the paper closes with conclusions in Section 7.

2 FIDO ROVER

The FIDO rover is an advanced technology rover that is a terrestrial prototype of the rover that NASA/JPL plans to send to Mars in 2003 (see <http://fido.jpl.nasa.gov>). FIDO's mobility sub-system consists of a six-wheel rocker-bogie suspension system [6] and is capable of traversing over obstacles up to 30 cm in height. FIDO is equipped with an analog of the science payload that the flight rover will carry.

FIDO has a 4-degrees-of-freedom (DOF) mast that extends to 1.94 m when deployed (as shown in Figure 1). When the vehicle is moving, the mast is stowed on the rover deck. The mast-head houses a stereo PanCam (panorama camera), a stereo NavCam (navigation camera), and an Infrared Point Spectrometer (IPS). The PanCam has a three-band near infrared imaging system capable of surveying the terrain in stereo with high spatial resolution for scientific purposes. The NavCam is a low spatial-resolution, monochrome, wide field-of-view stereo imaging system used for traverse planning. The IPS is bore sighted with NavCam and PanCam [7] and is used to acquire spectral radiance information in either a point or raster mode. In addition to the mast, FIDO has a 4-DOF Instrument Arm, a Mini-Corer, and BellyCam (a stereo camera) mounted on the underside or "belly" of the front of the rover. A color microscopic imager is mounted on the end-effector of the Instrument Arm. The Mini-Corer can be used to acquire sample cores from rocks of 0.5 cm diameter and up to 1.7 cm long. FIDO has two other sets of stereo cameras, called the Front HazCam and the Rear HazCam. The HazCams are used to provide range data for autonomous hazard avoidance algorithm for obstacle detection during rover traverses. The front HazCam is also utilized to choose science targets for in-situ instruments mounted on the Instrument Arm.



Figure 1 FIDO Rovers with the Mast and Instrument Arm Deployed at Black Rock

The rover-computing platform is a PC/104 266Mhz, Pentium-class CPU with a VxWorks 5.4 real-time operating system. FIDO uses three-layer software architecture: the lowest layer is the Device Driver Layer (DDL), the middle layer is the Device Layer (DL), and the top layer is the Application Layer (APL). The DDL handles all hardware dependencies (e.g., DIO, Counters, A/D drivers). The DDL provides the means for abstracting the higher-level software in the APL from the hardware dependencies. The DDL is responsible for all motion-control functions, vision processing, instrument interfaces, forward and inverse kinematics for the Mast and Instrument Arm, etc. The APL contains all rover sequences, instrument sequences, Sun sensor algorithm, and hazard-detection and path-planning software. The software on FIDO is written in ANSI-C.

FIDO has been used to simulate operational concepts for future Mars surface exploration missions. Recent field trials at Silverlake (1999) and the Soda Mountains (2001) in California's Mojave Desert, and at Black Rock Summit (2000) in Nevada's Great Basin helped shape the rover mission specifications outlined by NASA for 2003 mission to Mars. During these field trials, operations are directed from JPL by the actual Mars mission flight science team members and distributed collaborative users all over the world via the Internet. The Web Interface for Telescience (WITS) and the Multi-Mission Encrypted Communication System (MECS) are used for sequence planning and generation, and command and data product recovery (see <http://wits.jpl.nasa.gov>).

3 LONG RANGE NAVIGATION

Currently, planetary surface navigation is done by using waypoints that have been selected by ground operators from the mast imagery taken at the rover's current position. In order to drive farther than can be seen in these images, the rover must be able to autonomously plan paths and update its map as it moves. This section outlines the detailed concepts and formulation of the ROAMAN algorithm.

3.1 ROAMAN

The recently fielded ROAMAN algorithm uses a combination of long range path planning derived from imagery taken with mast-mounted wide baseline stereo cameras, and local path planning derived from body-mounted narrow baseline stereo cameras for autonomous long-range traverses. The long-range path planning portion of the system autonomously generates a series of waypoints that are passed to the local path planning algorithm (DriveMaps) for local obstacle avoidance during the traverse of the individual legs. Both portions of the algorithm use an occupancy grid representation to perform hazard detection and path planning. The algorithm is not guaranteed to generate an optimal shortest path, but will maintain the safety of the rover. The maps that are maintained by the higher and lower level portions of the system are not shared, since there may be substantial localization errors that accumulate during any long traverse.

There are two types of obstacles that would pose a threat to a rover: step discontinuities with a height greater than the body clearance of the rover, and slopes greater than 45 degrees, which are a tip-over hazard. A seven step algorithm is used to

build a traversability map from the raw range data derived from the mast and body mounted stereo cameras. The steps of the algorithm are:

1. Place range data into a discretely binned elevation map and interpolate small regions of missing data.
2. Compute the height distribution in each cell.
3. Compute the local surface normals by fitting planes to each cell and its neighbors.
4. Grow regions of similar slope.
5. Mark steep regions, discontinuities, and large regions of missing data as hazards.
6. Grow border around hazard cells to accommodate rover slippage and heading errors.
7. Mark the remaining cells as safe.

The traversability map generation process is similar to that used in [10]. These maps serve as the basis for all global and local path planning on the rover. The usable range for the global maps is about 12 meters, and that for the local maps is about 1 meter. These map sizes are dependent on the camera characteristics for the mast mounted NavCams and body mounted HazCams.

Each row of the discrete grid is then scanned and labeled for the center of the regions between all hazard cells on that line. This is equivalent to deriving the 1D medial axis or Voronoi transform for each row of the grid similar to that used in [12, 13]. The rover footprint is virtually driven on the paths as they develop in order to maintain safety in the event that a turn might be necessary. All labeled cells that fail this test are marked as unusable.

After the full grid has been scanned, a depth first search algorithm is run to find the longest connected paths. The previous step of the algorithm has eliminated most of the potential paths, so the search is very efficient since only cells labeled as safe path are included. Other search algorithms such as D* [6, 14] that are guaranteed to return the optimal path could also be run at this point. A least squares fit is done to the longest connected path in order to determine waypoints for the traverse. The FIDO rover performs turns-in-place followed by straight drives for the traverse in order to optimize rover power use.

4 LONG RANGE RENDEZVOUS

One of the scenarios for the Mars Sample Return (MSR) mission currently planned by NASA/JPL for 2013 calls for a science rover to egress from the lander to a number of remote sites possibly hundreds of meters away and acquire samples using a body mounted rock minicorer. The rover will then return to the lander for stowing of the samples onboard a solid fuel rocket prior to the rocket's launch into Mars orbit for later retrieval. Among the options that exist for this return to the lander are a radio beacon or visually guided traverse. In the event that power/mass constraints eliminate the radio beacon option, there is a need for the rover to autonomously return under visual guidance.

The navigation precision required for such a traverse varies depending on the distance from the lander. At distances greater than 40-50 meters, rough heading and range are all that is needed. In the 40-10 meter range, the rover must have some

sense of its pose and orientation relative to the lander. Within the 10 meter range, the rover must be able to precision align itself with the lander ramps prior to climbing back onto the lander deck. We have developed a three phase sequence that uses fusion of horizontal line and wavelet derived texture features for during the long-range, lander truss structure

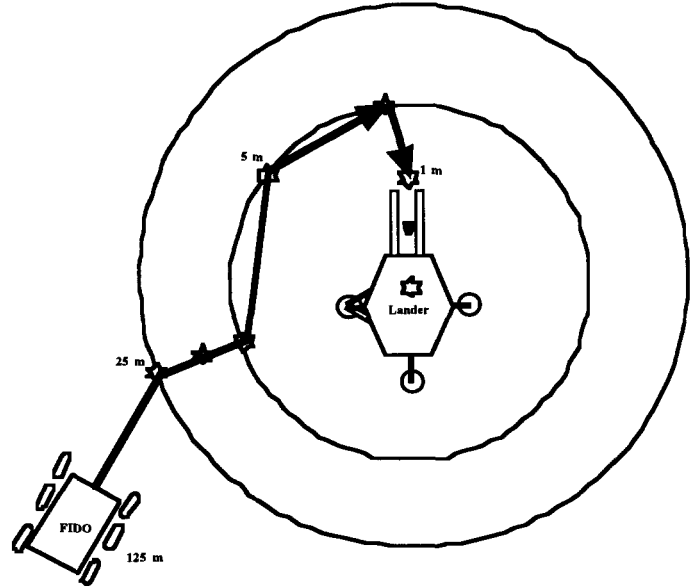


Figure 2. Three phase sequence for lander acquisition and rendezvous. See text for details.

features for the mid-range, and fiducial features on the lander ramps for the short-range portions of the traverse. This sequence is shown in Figure 2.

Visual acquisition of man-made structures such as a lander from long distances (125+ meters) in natural environments using single feature target recognition techniques tends to suffer from false positives due to lack of detail in the lander profile. The algorithm used in the long-range phase of the traverse uses line features (derived from Canny edge detection) fused with wavelet derived texture signatures [18] to eliminate false positives. This technique exploits spatial locality of the line and texture features for rapid lander localization in the mast mounted camera field of view. After the rover visually acquires the lander, the traverse is started with visual reacquisition of the lander every 5 meters. This mode of operation continues until the rover is within 25 meters of the lander based on fusion of wheel odometry data and visual angle sizing of the lander.

During the second phase, the rover traverses from 25 meters to a ramp standoff location of 5 meters. Since the relative distance is more important than absolute position during this phase, we use parallel line features visually extracted from the lander truss structure. In order to correctly distinguish the truss structure, the lander deck is detected first, which appears as a set of nearly leveled lines. Any parallel lines below the deck are considered as part of the truss structure. The average distance between the parallel pairs then is used to estimate the distance and the center of mass of these parallel lines is used to compute the heading direction.

During the third phase prior to climbing the ramps, the rover uses a distinctive pattern of stripes on the ramps to position itself within 10 centimeters of the base of the ramps. Once the rover is within the 5-meter range, it will circle around the lander. The close-range ramp alignment algorithm includes three major steps: feature extraction, feature match, and pose estimation. Features are the six stripes that were deliberately arranged on the ramps so that any two stripes have a unique combination spatially and topologically. This unique configuration greatly reduced uncertainty and computational complexity. An edge detection algorithm (Canny) is applied first. Then all straight-line segments are extracted. In order to find the stripes, we first look for the ramps, which are defined by a set of long straight and nearly parallel lines.

With a single detected stripe in the image, a linear affine transformation can be constructed based on the four corners. If this match is correct, the transformation can help to find other matches. Because there are relatively few stripes (six on the ramps), an exhaustive search is used to pick up the best match. Once the matches are found, the pose and orientation are estimated by using the outside corners of the stripes. A minimum of four stripes is used for safe navigation.

5 SINGLE COMMAND SCIENCE TARGET RENDEZVOUS

Three Martian days or sols are currently required to place a scientific instrument on a target. After the target is selected, a traverse to the target is plotted, the drive is performed, imagery is acquired, and finally, if the drive was successful, the instrument is deployed. The FIDO team has developed auto-approach technology for a single command sequence to autonomously perform these steps without ground intervention beyond the initial target selection. Feature points are derived onboard the rover using the image of the target taken from up to 6 meters away. These features are then tracked for docking and instrument arm deployment. Errors in odometry, which are typically anywhere from 6 to 30% due to varying terrain characteristics, are mitigated through this visual servoing technique during the rover approach.

The navigation and tracking portion of the algorithm consists of 14 steps:

1. At the starting location, a set of images are captured using the mast mounted NavCams. These images are used by the ground operators to select the position of a science target, which is then uplinked to the rover.
2. The rover faces this position using a turn-in-place and drives 1 meter using the DriveMaps algorithm described previously. At the second location, the mast is pointed at the target position and a second set of stereo images are taken.
3. The camera models for the first and second image pairs are transferred to the global coordinate frame according to the mast joint angles, rover attitude and position.
4. The Forstner interest operator [19] is run in a pre-defined region about the center of the initial left stereo image taken before the rover moved.
5. For each point returned by the operator, its epipolar line is computed based on the first and second camera models and range.

6. A strip of first image is projected along the epipolar line to the second image.
7. The rough location of this strip in the second image is determined using cross correlation [20].
8. A homography transform is applied to find the precise transform between the two images along this strip.
9. The location of this feature in the second image is computed using the homography transform.
10. The range of this feature is then recomputed at finest level in the stereo pyramid in order to obtain the best possible position.
11. The rover pose relative to the target is computed by applying steps 5 through 10 to all of features found step 4.
12. The final pose is transferred to the rover and the relative position of the target is corrected.
13. This gives the new drive target and mast pointing parameters for the next leg of the traverse.
14. The drive is performed and steps 2 through 13 are repeated until the rover is at the specified offset to the target for the science instrument deployment.

The target position used for instrument placement is derived from a range map that is generated using stereo images taken from as far as 10 meters away. These range maps typically have an uncertainty of about 1 to 2 %, which leads to an error of 3 or more centimeters in the target height and range. The range uncertainty is addressed through the auto-approach portion of the algorithm. We have developed and tested an algorithm that compensates for this uncertainty using wavelet texture features [18] to evaluate the focus of the color microscopic images. The instrument arm is moved down to the target in ten steps, with a focus calculation after each step. When the algorithm determines that the image is in focus, it is queued for downlink to Earth. If there is more than a 3 centimeter error in the estimated height of the target, the algorithm automatically predicts the correct placement distance for optimal focus. This auto-focus technique is integrated with the navigation and tracking portion of the auto-approach algorithm for a completely autonomous single command science target rendezvous and image acquisition process.

6 EXPERIMENTAL STUDIES

We have performed numerous field trials at locations in California's Mojave Desert, Nevada's Great Basin, and in the Arroyo Seco at JPL that have exercised the algorithms described above.

6.1 Long Range Navigation

We report preliminary results for the ROAMAN algorithm. The algorithm was run 3 times in the Arroyo Seco at JPL in a variety of rock field densities ranging from fairly benign to totally impassable. An example of the path plotted for rock field with medium density (15% obstacles/sq-m) is shown in Figure 3. The map generation process took 20 min to acquire the 37 pairs of stereo NavCam images. The path planning process took 250 millisecond.

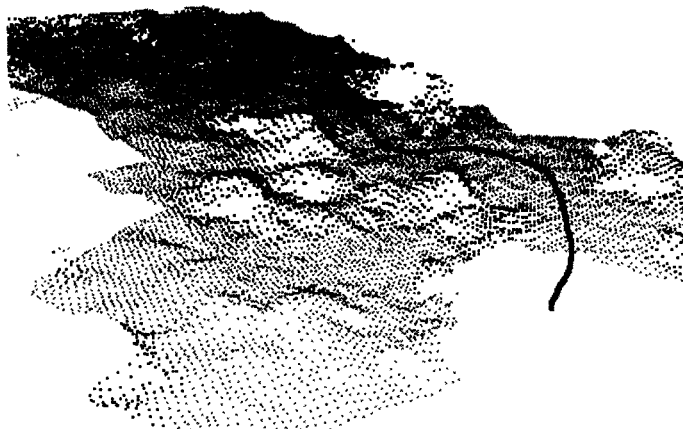


Figure 3. Long-range path planning for ROAMAN algorithm. The size of the grid is 6m by 12m (WXH) with a spatial resolution of 5cm per cell. Darker areas are hazard zones that include shadow regions unable to be imaged by the stereo cameras due to obstacles. The safe path is shown in red.

6.2 Long Range Rendezvous

The long range rendezvous algorithm was run at Black Rock Summit in Nevada's Great Basin, and in the Arroyo Seco at JPL using a mockup of the lander for the 2013 MSR mission. Some representative images of the final ramp approach at Black Rock Summit are shown in Figure 4. Figure 5 shows the performance of the fusion algorithm from a distance of 125 meters in the Arroyo Seco at JPL. The false positives (shown with boxed areas in the top frame) are totally eliminated after being fused with co-spatial horizontal line features. The extraction of features derived from the lander truss structure are shown in Figure 6, where the original image is shown on the top, and the visually extracted features are shown on the bottom. The average distance errors to the lander for 15 runs of the algorithm are 0.86% at 15 meters, 2% at 25 meters, 9.6% at 35 meters, and 6.2% at 45 meters. Extraction of stripes on the lander for the close-range approach is shown in Figure 7, where the original image is shown on the top, and the visually extracted features are shown on the bottom. The average error in placement for the rover in relation to the ramps for 15 runs was 1.8cm in the lateral and 2.4cm in the longitudinal directions, with a average heading error of 2.7 degrees.

6.3 Autonomous Science Target Rendezvous

The auto-approach algorithm was run 5 times in the Arroyo Seco at JPL. The targets at an average distance of 5.9 meters from the initial position of the rover were selected remotely using the WITS interface. Some representative images from the mast mounted NavCams with the tracking features marked by crosses are shown in Figure 8. The average placement error for these runs was 7.5cm, which corresponds to a 1.3% error. The average measured error for the distance traveled according to wheel odometry over the same terrain was 92.63cm, which corresponds to a 15.7% error. A comparison of the these two

methods indicates that the majority of the error was largely eliminated due to the feature tracking used in the auto-approach algorithm.

The auto-focus algorithm was run 50 times on a variety of rock and soil targets in the remote sites during the course of the field trials. It correctly predicted the optimal focus in 100% of the soil targets, and 82% of the rock targets. An example of its performance for a soil target is shown in Figure 9. The errors in the rock target predictions can be traced to the triggering of the contact sensor on the color microscopic imager as it came in contact with the edge of a rock, which gives a partially out-of-focus image.

7 CONCLUSIONS

In this paper, we have presented algorithms that greatly increase rover autonomy for long-range navigation and rendezvous with both man-made and natural targets. These algorithms were implemented and tested on the FIDO rover, a technology prototype for the dual Mars Exploration Rovers being sent to Mars in 2003. The algorithms ran within the computing constraints of the platform (266 MHz Pentium, 64MB RAM) with the longest delays (6 sec) being taken by the stereo image processing. These algorithms greatly increase the science return for planetary missions due to the decrease in the number of sols necessary for navigation to and instrument placement onto targets. In addition, we demonstrated in the field, a long-range rendezvous algorithm that is suitable for a return-to-lander MSR sequence using visually guided navigation and precision alignment with ramps.

We are currently investigating the incorporation of higher resolution cameras in an effort to increase the range for autonomous navigation and target acquisition. In addition, the inclusion of the accelerometer data and feature tracking in the HazCam images during traverses into the EKF state estimation process will further refine the odometry estimates. The desired science instrument placement accuracy is 2cm from a distance of 10 meters, which is theoretically feasible with cameras that are commercially available with double the spatial resolution (1024X1024) to those we currently use.

8 ACKNOWLEDGMENT

This research was carried at the Jet Propulsion Laboratory, California Institute of Technology, under a contract with the National Aeronautics and Space Administration. We would like to express our sincere appreciation to all of the members of the FIDO Rover team who have contributed to the successful technology development and field trials during the past three years.

9 REFERENCES

1. E. Gat, M. Slack, D. Miller, and R. Firby, "Path planning and execution monitoring for a planetary rover," *Autonomous Mobile Robots: Control Planning and Architectures*, Iyengar and Elfes, Eds., IEEE Computer Society Press, 1991.
2. E. Rimon and J. Canny, "Construction of C-space roadmaps from local sensory data: What should the

- sensors look for?" in *Proc. IEEE Int. Conf. on Robotics and Automation (ICRA'94)*, San Diego, CA, pp. 117-123, 1994.
3. A. Trebi-Ollennu, T. Huntsberger, Y. Cheng, E. T. Baumgartner, B. Kennedy and P.S. Schenker, "Design and Analysis of a Sun Sensor for Planetary Rover Absolute Heading Detection," *IEEE Trans. Robotics and Automation*, 2001, to appear; also tech report NASA CR-2001-210800, Jet Propulsion Laboratory, California Institute of Technology.
 4. R. Volpe, "Mars rover navigation results using sun sensor heading determination," in *Proc. IEEE/RSJ International Conference on Intelligent Robot and Systems*, vol. 1, pp. 460-467, 1999.
 5. I. Kamon, E. Rivlin, and E. Rimon, "Range-sensor based navigation in three dimensions," in *Proc. IEEE Int. Conf. on Robotics and Automation (ICRA'99)*, Detroit, MI, pp. 163-169, 1999.
 6. A. Yahja, S. Singh, and A. Stentz, "An efficient on-line path planner for outdoor mobile robots operating in vast environments," *Robotics and Autonomous Systems*, 33(2&3), 129-143, Aug 2000,.
 7. E.T. Baumgartner, "In-Situ Exploration of Mars Using Rover Systems," in *Proc. AIAA Space 2000 Conference*, AIAA Paper # 2000-5062, 2000.
 8. E.T. Baumgartner, H. Aghazarian, A. Trebi-Ollennu, T.L. Huntsberger, and M.S. Garrett. "State Estimation and Vehicle Localization for the FIDO Rover," in *Proc. SPIE Conf. Sensor Fusion and Decentralized Control in Autonomous Robotic Systems III*, vol. 4196, Boston, MA, pp. 329-336, Nov 2000.
 9. E. T. Baumgartner, H. Aghazarian, and A. Trebi-Ollennu, "Rover localization results for the FIDO rover," in *Proc. SPIE Conf. Sensor Fusion and Decentralized Control in Autonomous Robotic Systems IV*, vol. 4571, Newton, MA, Oct 2001.
 10. S. Singh, R. Simmons, M.F. Smith, III, A. Stentz, V. Verma, A. Yahja, and K. Schwehr, "Recent progress in local and global traversability for planetary rovers," in *Proc. IEEE Int. Conf. on Robotics and Automation (ICRA'00)*, San Francisco, CA, 2000.
 11. B. D. Hoffman, E. T. Baumgartner, T. L. Huntsberger, and P. S. Schenker, "Improved rover state estimation in challenging terrain," *Autonomous Robots*, Vol. 6, pp. 113-130, 1999.
 12. S. A. Wilmarth, N. M. Amato, and P. F. Stiller, "MAPRM: A probabilistic roadmap planner with sampling on the medial axis of the free space," in *Proc. IEEE Int. Conf. on Robotics and Automation (ICRA'99)*, Detroit, MI, pp. 1024-1031, 1999.
 13. H. Choset, *Sensor Based Motion Planning: The Hierarchical Generalized Voronoi Graph*, Ph.D. thesis, California Inst. of Tech., 1996.
 14. A. Stentz, "Optimal and efficient path planning for partially-known environments," in *Proc. IEEE Int. Conf. on Robotics and Automation (ICRA'94)*, 1994.
 15. S. Singh and B. Digney, *Autonomous Cross-Country Navigation Using Stereo Vision*, tech. report CMU-RI-TR-99-03, Robotics Institute, Carnegie Mellon University, January, 1999.
 16. S. L. Laubach, J. W. Burdick, and L. H. Matthies, "An autonomous path-planner implemented on the Rocky7 prototype microrover," in *Proc. IEEE Int. Conf. on Robotics Automation (ICRA'98)*, 1998.
 17. S. L. Laubach and J. W. Burdick, "An autonomous sensor-based path-planner for planetary microrovers," in *Proc. IEEE Int. Conf. on Robotics and Automation (ICRA'99)*, Detroit, MI, pp. 347-354, 1999.
 18. F. Espinal, T.L. Huntsberger, B. Jawerth, and T. Kubota, "Wavelet-based fractal signature analysis for automatic target recognition," *Optical Engineering, Special Section on Advances in Pattern Recognition*, 37(1), 166-174, 1998.
 19. Fortsner and Pertl, *Photogrammetric Standard Methods and Digital Image Matching*, 1986.
 20. C. F. Olson, L. H. Matthies, M. Schoppers, and M. W. Maimone, "Robust stereo ego-motion for long distance navigation," in *Proc. IEEE CVPR*, Hilton Head, SC, pp 453-458, June 2000.



Figure 4. Final lander ramp approach by FIDO rover at Black Rock Summit in Nevada's Great Basin (Map 2000). Rover has traversed from 15 m away and in the center frame is using the mast mounted PanCams for a final heading adjustment.

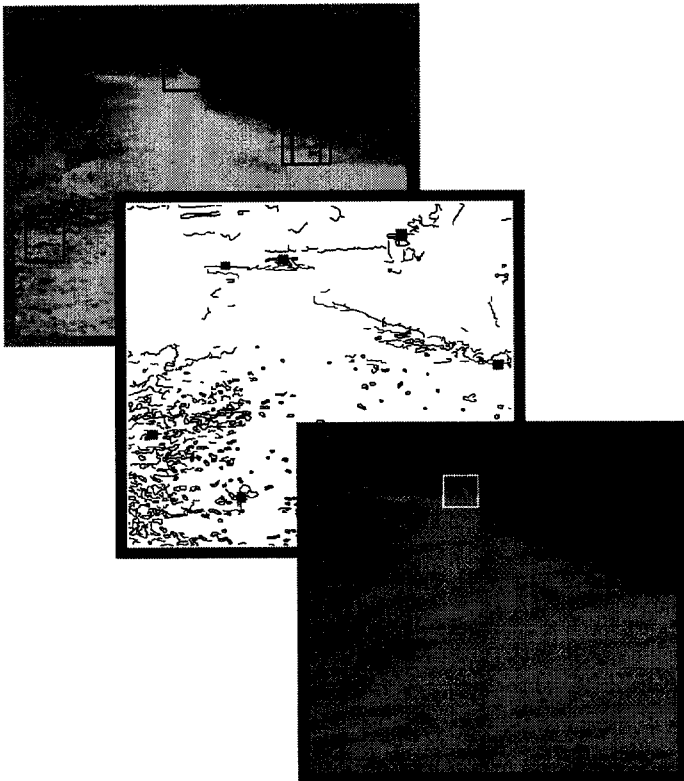


Figure 5. Long-range (125m) identification of lander using a multi-feature fusion process. Top: Boxed areas are potential lander positions returned by wavelet texture operator; Middle: Red squares are potential lander positions based on collections of horizontal lines; Bottom: Co-

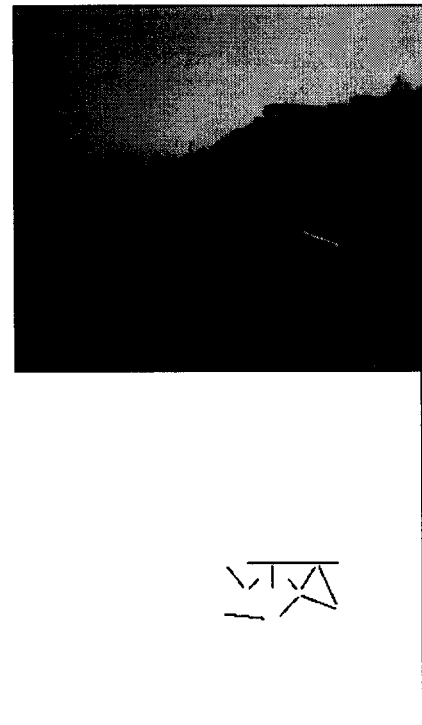


Figure 6. Mid-range feature extraction using line detection followed by lander geometry constraint satisfaction. Top: Original image; bottom: extracted truss and lander top features.

Figure 9. Wavelet texture focus index for microscopic images of target taken at ten steps of 3 mm each. Vertical axis is value of index, and horizontal axis is the distance to the target starting on the left from 3 cm away.

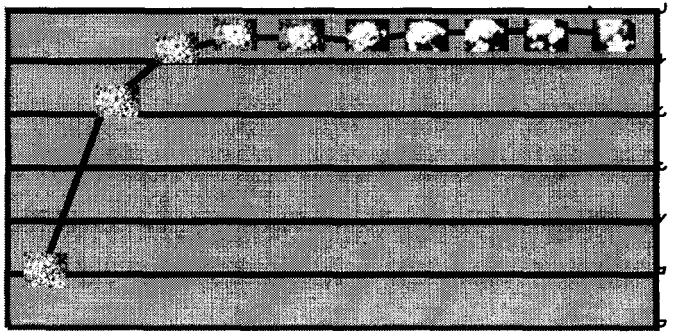


Figure 7. Close-range feature extraction of line elements that are used for stripe identification on the lander ramps.

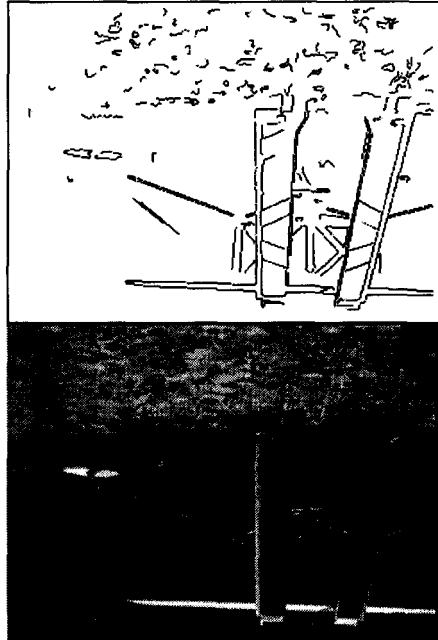


Figure 8. Feature tracking for auto-approach. Features are shown as crosses, with the science target shown with an arrow in each image. Top: range is 2.7 meters from the science target; Bottom: range is 1.7 meters from the science target.

